Asociación Argentina
de Mecánica Computacional

Mecánica Computacional Vol XXXIX, págs. 1297-1306 (artículo completo)
F.E. Dotti, M. Febbo, S.P. Machado, M. Saravia, M.A. Storti (Eds.)
Bahía Blanca, 1-4 Noviembre 2022

A NOVEL DFT STUDY OF QUANTUM CAPACITY AND ELECTRONIC STRUCTURE OF 2D MATERIALS FOR LI-ION BATTERIES

Julian Juan[a,b], Pablo Bechthold[a,b], Maria J. Jiménez[a,b], Francisco Gaztañaga[a,b] , Graciela P. Brizuela[a,b], Paula V. Jasen[a,b], Ricardo Faccio[c] and Estela A. González[a,b]

[a]*Grupo de Ciencia de Materiales Computacional, Dpto. Física, Universidad Nacional del Sur, Av. Alem 1253, 8000 Bahía Blanca, Argentina*

[b]*Grupo de Ciencia de Materiales Computacional, IFISUR, CONICET, Av. Alem 1253, 8000 Bahía Blanca, Argentina*

[c]*Grupo de Ciencia de Materiales y Nanotecnología, Facultad de Química, DETEMA, UDELAR, Av. Gral. Flores 2124, 11800 Montevideo, Uruguay*

Keywords: DFT, Quantum Capacity, Electronic Structure.

Abstract. 2D materials have a wide surface and unique electronic properties as compared to bulk materials. Due to the high stability, high abundance, and the existence of an excellent compatible oxide, Si and Si-based layered materials are the leading ones for microelectronic devices and may be the most promising materials for realistic applications. Lithium-ion batteries (LIBs) have become the most successful type of energy-storage device for applications ranging from portable electronic devices to modes of transport such as electric vehicles, due to their lightweight, environmental friendliness, and high energy density. Si-based 2D materials, unlike metals, do not have a good screening. Therefore, it is expected that their intrinsic capacitance has a prominent influence on the performance of devices when these materials are used in electrodes. We performed DFT calculations of Li^q adsorption (q = -1, 0 or +1) on a silicene single layer. Pristine and defective silicene configurations with and without Li doping were studied: single vacancy (SV), double vacancy (DV) and Stone-Wales (STW). Quantum capacity (QC) and charge density studies were performed on Li adsorbed in various sites of the substrate. Moreover, structural studies, adsorption energies, electronic structure and charge density difference analysis were performed before and after adsorption at the most stables sites, which showed the presence of a magnetic moment in the undoped SV system, the displacement of the Fermi level produced by Li doping and a charge transfer from Li to the surface. The QC analysis showed that the generation of defects and doping improves the QC of silicene in positive bias, because of the existence of 3p orbital in the zone of the defect. Consequently, the innovative calculations performed in this work of charged lithium doping on silicene can be used for future comparison with experimental studies of this Li-ion battery anode material candidate.

1 INTRODUCTION

Currently, 2D materials with high surface area, high power density, high stability and high conductivity are highly demanded as electrode materials in metal-ion batteries (Wang et al., 2012). The demand for portable energy sources is currently increasing and improvements in Li-ion batteries (LIBs) have become an important quest. The conventional material used as the anode is graphite, but a new alternative are the 2D graphene-like forms such as silicene and others (Ayodhya y Veerabhadram, 2020). Therefore, understanding the formation and migration of defects as well as their influences on the electronic/magnetic properties of these novel 2D materials not only is meaningful for fundamental research, but also provides a powerful route to customize their physical properties and to control their functional applications in future devices.

Due to the high stability, high abundance, and the existence of an excellent compatible oxide, Si and Si-based layered materials are the leading ones for microelectronic devices and may be the most promising materials for realistic applications (Luo et al, 2014; Yu, 2018). In the large family of 2D materials, silicene deserves a special consideration because of its compatibility and expected integration with current nanotechnology. Silicene is a silicon counterpart of graphene with a tiny band gap of 1.55 meV (Chowdhury y Jana, 2016). This 2D material has the distinctive property of a buckled honeycomb structure, allowing better interactions of this surface with Li atoms, and therefore is advantageous for application in Li-ion batteries. Hawever, lower energy density of silicene-based materials severely limits its implementation. Many attempts are being made to increase materials capacitance performance (Chavan et al, 2018), and enhancing quantum capacitance is one of the most effective techniques to generate materials with high energy density (Zhang et al., 2012). To that end, we analyze the effect, to the quantum capacity, of adsorbing a Li atom with different initial charge states to a pristine and a defective silicene layer.

2 METHODOLOGY

We used Density Functional Theory based calculations, implemented with the VASP code (https://www.vasp.at/). We computed the optimized geometrical structures and electronic properties of pristine and defective silicene, with the projector augmented wave potentials methods applied. Periodic plane waves and Blöch's projector augmented wave (PAW) are used in order to obtain the description of the valence electronic states and the core-valence interaction, respectively (Blöchl, 1994). The Perdew-Burke-Ernzerhof (GGA-PBE) parameterization is utilized in order to obtain the exchange-correlation energy of interacting electrons (Perdew, 1996). The valence electron configurations are $1s^2\ 2s^1$, [Ne] $3s^2\ 3p^2$ for Li and Si, respectively. A kinetic energy cutoff of 700 eV, and a 7x7x1 k-point mesh within the Monkhorst-Pack method are used (Monkhorst y Pack, 1976). A smearing parameter of 0.05 eV is used within the Methfessel-Paxton method. The convergence criteria for optimizations are 0.02 eV/Å for forces and 1×10^{-4} eV for total energy change. Stress tensors elements reached down to 1.0 kbar for the optimization of cell parameters. The possible magnetism of the defective system is considered with the implementation of spin polarized calculations. Based on lattice parameters of the primitive cell, we construct a supercell of 5x5 units with hexagonal structure. A vacuum of 11 Å along the z direction is considered, in order to prevent the artificial interaction between layers. All structural models are fully relaxed. We considered three possible charge states (q = +1, 0 and −1) for the Li adsorption on the systems. The adsorption energy is calculated using the following equation:

$$E_{ad} = E_{Li^q} + E_{system} - E_{system+Li^q} \quad (1)$$

where q represents the Li atoms charge, E_{Li^q} is the energy of a single charged Li atom, E_{system} is the pristine or defective silicene total energy and $E_{system+Li^q}$ is the total energy of the system after the adsorption. The defect formation energy is calculated according to:

$$E_{df} = E_{dsystem} - \frac{N-1}{N} E_{system} \tag{2}$$

where, E_{df} represents the formation energy of the system with the defect, $E_{dsystem}$ is the energy of the defective silicene, and N represents the number of Si atoms in the configuration. When both the volume and entropy effects are neglected, the open circuit voltage (OCV) can be obtained using the following equation (Wang y Li, 2020):

$$OCV \approx \frac{-E_{system+Li^q} - (E_{Li^q} + E_{system})}{e} \tag{3}$$

where, $E_{system+Li^q}$ and E_{system} represent the adsorption energy of lithiated and nonlithiated systems, respectively. E_{Li^q} is the Li atom cohesion energy in bulk BCC crystal and e is the electron charge.

The quantum capacity is calculated according to the work of Paek (Peak et al., 2013) by:

$$C_Q = e^2 \int_{-\infty}^{+\infty} D(E) \frac{sech^2((E-e\Phi)/2k_BT)}{4k_BT} dE \tag{4}$$

where D(E) is the density of states, ϕ is the local potential, E is the relative energy with reference to the Fermi level, e is the elementary electric charge and k_B is the Boltzmann constant. In all calculations the T was set to 300 K.

In silicene, the Si atom has a hexagonal crystalline arrangement in a $P\underline{3}m1$ space group, with a unit cell formed by two Si atoms. Our calculated values for the lattice parameter, bond length, buckling height and angles were a = 3.87 Å, Si-Si = 2.28 Å, Δz = 0.44 Å, α = 90º, β = 90º and γ = 60º, which are in good agreement with those reported in the literature (Huang et al., 2013). To simulate the charged Li atom adsorption with a concentration of x(Li) = 0.02, a supercell of 5 x 5 surface of 50 atoms was constructed. In all the calculations, the lateral displacement of the Li atom is restricted. The van der Waals calculation is tested in the pristine case for Li atom adsorption, finding an energy difference of 0.03 eV in comparison with the case without considering the long-range interaction. Therefore, the van der Waals interactions are not considered in the calculations.

3 RESULTS AND DISCUSSION

3.1 Geometry and systems energetic stability after Li adsorption

In this work, pristine and defective silicene is studied, where the defective systems are silicene with a single vacancy (SV), a double vacancy (DV) and a Stone-Thrower-Wales (STW) defect. The obtained E_{df} values are 3.40 eV, 3.73 eV and 2.09 eV for SV, DV and STW configurations, respectively. These formation energies are in good agreement with those reported by Setiadi et al., 2013.

For charged Li^q (q = -1, 0, +1) adsorption, the high symmetry adsorption sites are considered: top, bridge and hollow (see inserts on Figure 1 a-d). In these figures, H is a 6-fold hollow site in the perfect zone (PZ), while H1 and H2 are a 6-fold hollow and a 5-fold pentagonal hollow site in the defect zone (DZ). The T, V, B, T1, V1 and B1 represent a top on a superior silicon atom, a valley (top an inferior Si atom) and 2-fold bridge sites in the perfect and defect zone, respectively. The defect sites are labeled SV (single vacancy), DV (double vacancy) and STW (Stone-Thrower-Wales), depending on the defective system.

Table 1 summarizes the calculated adsorption energies, Li-Si bonds and OCV at the most favorable sites for all the doped configurations of the Li_xSi sheet. The adsorbed configurations are presented in the inserts-on Figs. 2 and 3. It can be seen that Li^{-1} ion for the most stable configurations has smaller adsorption energy values for all systems, therefore we decide only to consider the Li^0 and Li^{+1} for the further analysis. In all adsorbed systems, the hollow sites present higher energy values. Except in the case of silicene with a single vacancy, where the Li prefers to be located in the defect site SV, which is, overall, the most stable one for the Li adsorption on the surface. This is in good agreement with the results reported by Setiadi et al., 2013. Also, it is important to remark that in the defective system the most stable hollows are those closest to the DZ. The energy trend is SV (SV configuration) > H2 (STW configuration) > H2 (DV configuration) > H (pristine configuration), which is related to the electrostatic interaction between the adsorbate ion and the defective substrate. This is in good agreement with the results reported by Pattarapongdilok and Parasuk, who considered the same charged states of lithium on graphene quantum dots (Pattarapongdilok y Parasuk, 2020). The results show that positive charged Li adsorption energy is the highest in all cases, which is consistent with a more realistic experimental situation.

	E_{ad} (eV)			Li-Si (Å)			OCV (V)		
Structure/Site	q			q			q		
	-1	0	+1	-1	0	+1	-1	0	+1
Pristine									
H	-1.20	-2.16	-4.29	2.67	2.69	2.72	1.20	2.16	4.29
Defected - SV									
SV	-2.96	-3.31	-4.81	2.51	2.54	2.49	-2.96	3.31	4.81
H1	-2.82	-3.22	-4.79	2.62	2.65	2.68	-2.82	3.22	4.79
Defected - DV									
DV	-2.67	-2.88	-4.30	2.69	2.69	2.68	2.67	2.88	4.30
H2	-2.10	-2.58	-4.32	2.66	2.68	2.68	2.10	2.58	4.32
Defected - STW									
STW	-1.83	-2.46	-4.41	2.60	2.61	2.71	1.83	2.46	4.41
H2	-1.88	-2.47	-4.48	2.61	2.63	2.69	1.88	2.47	4.48

Table 1: Adsorption energies (eV), Li-Si bond lengths (Å) and OCV (V) calculated values for charged Li atom adsorbed at the most stable sites in pristine and defected silicene.

After adsorption, the shorter and larger Li-Si bond distance corresponds to an H site for Li^{+1} on pristine silicene, and SV site for the Li^{+1} on silicene with a single vacancy, respectively. The OCV for Li^{+1}-doped systems in all considered cases are higher than pristine silicene. For the defected silicene, the average OCV for all q follows the trend SV > DV > STW (> pristine), except for q = +1 in the DV system, which has a lower value than the STW one. The highest OCV in all systems is that for q = +1, suggesting that doping silicene with Li^{+1} could be a suitable strategy for Li dispersing in LIBs electrodes.

The obtained OCV values for defected silicene are higher than the corresponding values for N-doped (Yu, 2013a) graphene and graphenylene (Yu, 2013b), which makes silicene an excellent material for enhancing battery performance.

3.2 Electronic structure, Bader analysis and quantum capacity

Regarding the electronic structure, the projected DOS, Quantum capacity and Charge density vs local electrode potential for pristine and defective silicene are shown in Figure 1. Except for the case of silicene with an SV, which presents asymmetric spin up and spin down contributions to the DOS with a magnetic moment of 1.85 μ_B, all the other cases present symmetric contributions (see the upper insert on the left in Fig. 1b). Only the spin up contribution is plotted. These results are in good agreement with those reported by Ali et al., 2017. It can be seen from Figure 1a on the left, that the pristine silicene shows a semiconductor behavior, with intersecting conduction and valence bands at the Fermi level (E_F). In the cases of SV and DV systems, the defect states give rise to localized states around the Fermi Level, shifting the E_F down into the VB and giving a metallic character to this defective silicene (see Figs. 1b and c, left). This is consistent with a p-doping behavior. For silicene with the STW defect, no changes can be observed in the PDOS curves when it is compared with the pristine case (compare Figs. 1a and d, left side).

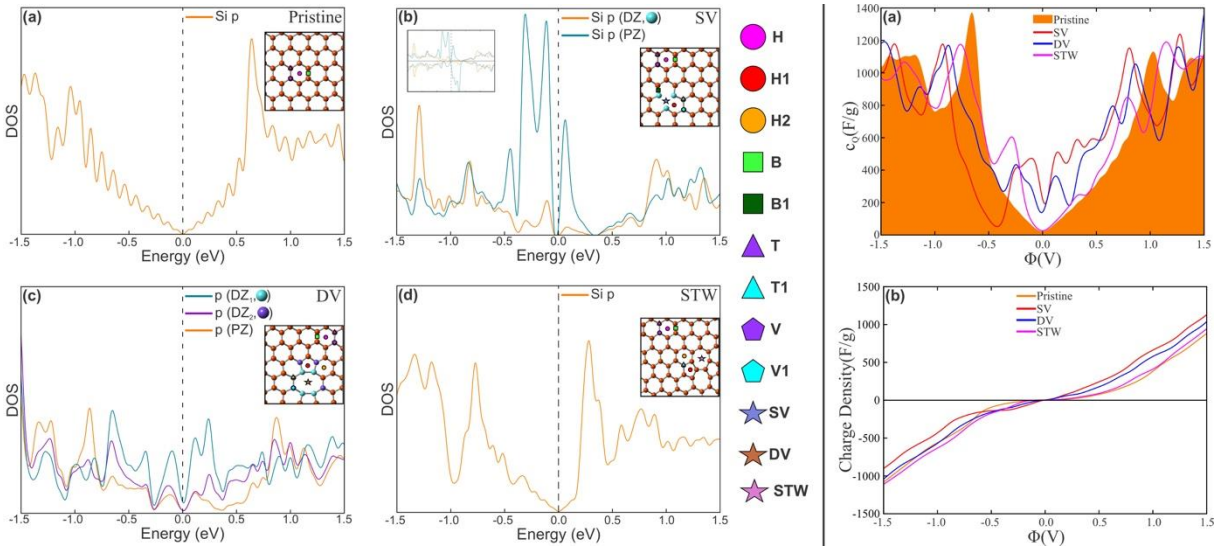

Figure 1: Projected DOS curves for pristine (a) and defective (b-c) silicene (left). Inserts present schematic views of systems with the possible adsorption sites. The upper insert on the right on Figure b is the spin polarized PDOS around the Fermi level (0 eV) for the SV system. The orange spheres represent Si atoms on the perfect zone (PZ), while the light blue and violet are those in the defective zone (DZ). Quantum capacity vs local electrode potential (a) and Charge density vs local electrode potential (b) for the pristine and defective systems (right).

In the right side of Figure 1 the calculated QC and charge densities vs local electrode potential of the pristine and the defective configurations are shown. The QC for the pristine case presents a maximum at approximately -0.6 V (orange area in Fig. 1a, right side). Also, it shows the lowest curve in the positive charge zone (see orange curve in Fig. 1b, right), which is consistent with the few states around the E_F on the PDOS curves (Fig. 1a, left). These results are in good agreement with those reported by Momeni et al., 2020; Yang et al., 2018; Xu et al., 2019. The Dirac point is shifted to the left, near -0.5 V and the charge density shows a predominance in the positive charge zone while it is less predominant in the negative zone for the SV configuration (see red curve in Fig. 1b, right). This is a consequence of the important number of defect states around the E_F (see Fig. 1b. left), which improved the QC in comparison to the pristine case. For the DV system the minimum in QC curve remains closest to 0 V, while the charge density curve is the second most predominant in the positive zone (see blue line in

Fig. 1b, right). This behavior is due to the defect states below the Fermi level, which come mainly from the atoms in the DZ1 (see Fig. 1c, left). These results agree with those reported by Yang et al., 2018. The PDOS curves of STW systems have the same behavior that the pristine case, then the QC curve of both systems are very similar. Also, the charge density vs Φ plot shows that the curve for STW configurations is the predominant one in the negative zone (see Figs. 1a, d left and the dark pink line in Figs. 1a and b, right). Similar results are reported by Momeni et al., 2020. In summary, these results show that the 3p orbitals of Si atoms in defective zones produce an improvement on charge density in the positive voltage zone and an enhancement of QC of silicene in positive bias, which is necessary for better supercapacitors.

The projected DOS (left), Quantum capacity and Charge density vs local electrode potential (right) for pristine and defective silicene after charged Li adsorption in the most stables site are shown in Figures 2 and 3 (only spin up contributions are presented due to symmetry). When Li^0 atom adsorbed at an H site on pristine silicene, the hybridization between Li s and Si p orbital produces a shift to the right in the Dirac cone, which is consistent with an n-type doping character (see Fig. 2a, right). While in the case of the Li^{+1} adsorption at the H site, it can be seen in Figure 2b (left) that the PDOS curves behavior is similar to the curves in the undoped system. For the Li atom adsorbed at the STW site of STW configurations, the DOS curves show a metallic behavior due to a strong hybridization of s-p orbitals of Li-Si interaction, while there are almost no changes on the projected DOS around E_F when Li^{+1} is adsorbed. At the H2 site on this system, the Li^0 atom introduces changes in the end of valence band due to Li s orbitals and Si p orbitals hybridization between -0.5 eV and the E_F, while in the case of Li^{+1} ion, the E_F is at the beginning of the conduction band (see Figs. 2c-f, left).

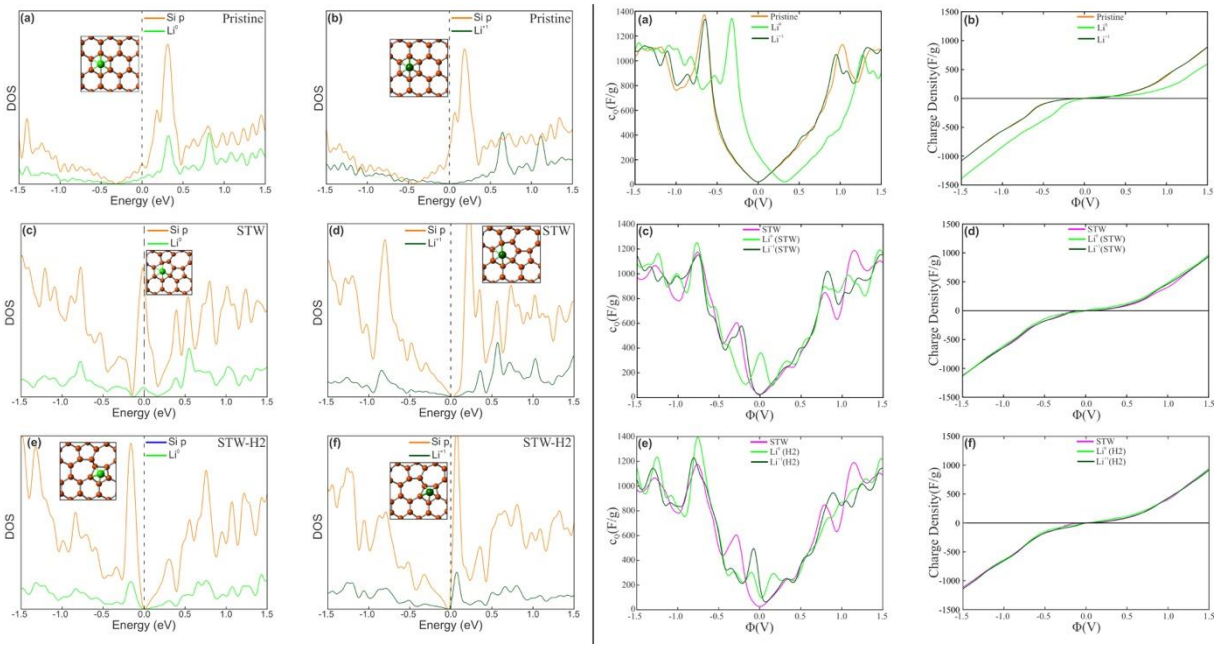

Figure 2: Projected DOS curves for Li atom and Si nearest neighbor atoms to the adsorbed site on pristine (a, b) and STW (c-f) systems after charged Li atom adsorption at the most stable sites (left). The Li PDOS curves are magnified for a better view. Inserts present a schematic view of the adsorbed systems. The orange, light green and dark green spheres indicate the Si atom, the Li^0 atom and the Li^{+1} ion, respectively. Quantum capacity and Charge density vs local electrode potential for pristine (a, b) and STW (c-f) defective silicene with and without Li adsorption at the most stable sites (right). The Fermi level corresponds to zero energy.

In Figure 2a (right) it can be seen a displacement of the quantum capacity to positive values (which is consistent with the shifts of the E_F presented in the PDOS in Fig. 2a, left) and also an

enhancement of QC in negative biases when the Li^0 adsorbed at the H site, while the Li^{+1} ion does not produce an increase in the QC and is similar to the pristine case, which agrees with behavior of the PDOS after the adsorption (see Figs. 2a on the right and 2b on the left side). The charge density curves in Figure 2b (left) are identical to that in the pristine system for the Li^{+1} case, while for the Li^0 doped system a predominance in the negative charge density zone is shown. For Li adsorbed at the STW site of the STW system, the QC shows a small enhancement in the Li^0 case in the positive voltages, which is consistent with some presence of states below the E_F in PDOS curves. The Li curves show a positive displacement for Li^0, while no displacement is present in the case of Li^{+1} (see Figs. 2c on the right and 2c-d on the left side). In Figure 2d (right), the charge densities curves are almost all superimposed, being the most positive the one corresponding to the Li^0. In the case of Li adsorbed at the H2 site on the STW system, Figures 2e and f (right) show a general shape similar to Figures 2c and d (right) and there is no noticeable enhancement and displacement of the curves.

For the Li^0 and Li^{+1} adsorption at the most stable sites on SV system, the Fermi level is shifted to lower energies showing a p-type doping character as consequence of the s-p hybridization in the Li-Si interaction. The main difference is the shift, which is consistent with a different amount of charge transfer in both cases (see Figs. 3a-d, left). In the case of the DV system after Li^0 is adsorbed, for both adsorption sites, the strong hybridization of Li s and Si p orbitals of the states around the Fermi level generate a metallic behavior in the DOS curves. The same behavior, with a different shift, is present in DOS curves when Li^{+1} is adsorbed at the DV site. For Li^{+1} adsorbed at the H2 site, the E_F is shifted to the end of the VB due to the s-p orbitals hybridization of Li and Si atoms near the Fermi level (see Figs. 3e-h, left).

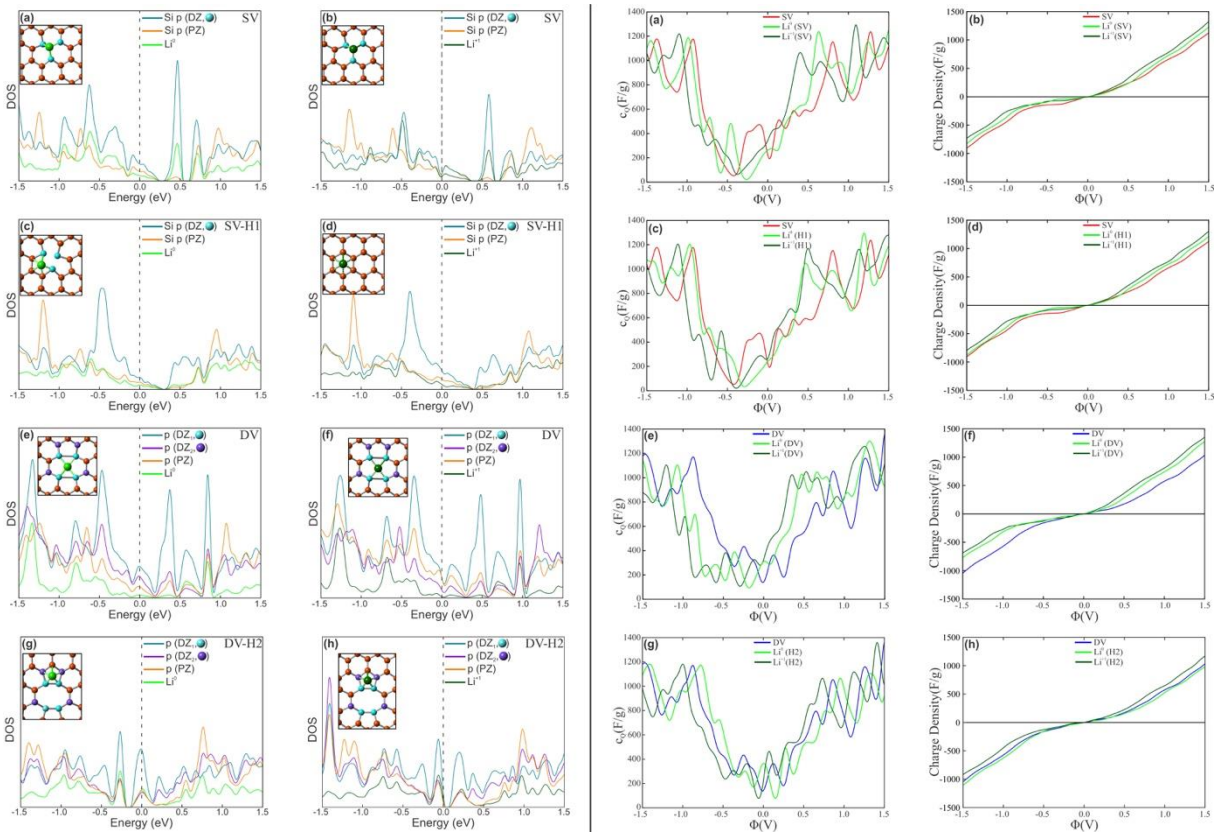

Figure 3: Projected DOS curves for Li atom and Si nearest neighbor atoms to the adsorbed site on SV (a-d) and DV (e-h) systems after charged Li atom adsorption at the most stable sites (left). The Li PDOS curves are magnified for a better view. Inserts present a schematic view of the adsorbed systems. The orange, light blue and violet spheres indicate the Si atom in the PZ and in the DZ, respectively. While the light green and dark green

spheres represented the Li^0 atom and Li^{+1} ion. Quantum capacity and Charge density vs local electrode potential for SV (a-d) and DV (e-h) defective systems with and without Li adsorption at the most stable sites (right). The Fermi level corresponds to zero energy.

For the QC in the case of the doped SV configurations, it can be seen that the adsorption of charged Li at the most stable sites produces an increase in the maximum of the quantum capacitance, which is consistent with more positive states below the E_F of the PDOS, which generate an increase of the positive QC. The displacement of the graphs shows that the Li^{+1} adsorbed configurations have its minimum near the SV case, while the Li^0 configurations are displaced to the right. The charge density shows that the Li^{+1} systems have the most positive charge densities (see Figs. 3a-d on the right and a-d on the left side).

Comparing the DV system before and after adsorption of charged Li, an increase in QC in positive voltage values is present (compare Fig. 1a with Figs. 3e and g, both on the right side), which can be related to more states below the E_F in the PDOS curves (see Figs. 3e-h, left side). For Li^0 and Li^{+1} adsorbed at the DV site, the minimum is shifted to negative values, while in the case of Li adsorbed at the H2 site, the minimum is again almost at 0 V for Li^{+1} and moved to positive values for Li^0 (see Figs. 3e and g, right side). Again, an increase in the QC for the different cases is observed. At the positive voltages, the Li^{+1} curve shows an enhancement, while the Li^0 curve shows an enhancement in the negative voltages. The charge densities show that the Li^{+1} case is the most positive one (see Figs. 3f and h, right side). These results are consistent with the behavior of the PDOS around the Fermi level for the different DV configurations (see Figs. 3e-h, left side).

Summarizing, the doping produces an enhancement in the quantum capacities and charge densities. These results are useful to analyze these systems for future application. Also, it can be noted that the Li doping with different charge values have an effect in the displacement for these curves. A significant increase in the positive voltages in the QC is present, mostly for the Li^{+1} cases on SV and DV doped sites. The responsible for these changes are the 3p orbitals of Si atoms in defective zones. The case of the H2 site on the STW doped system shows the small enhancement in QC.

In all the considered systems, Bader charge analysis [23] at the most stable adsorption sites show that Li^{+1} ion has a final charge of about +0. $9e^-$, indicating the existence of a small charge transfer to the surface. In the case of Li^0 atom, the charge transfer to the surface is about $0.9e^-$. This is due to the sp hybridization of the Li-Si bond and is consistent with a cationic behavior of Li atom and anionic character of the surface. Charged and a neutral Li. Similar behavior is reported for Li^+ ion adsorbed on pristine and defective graphene sheets (Shanmugam et al., 2020; Sangavi et al., 2019)

4 CONCLUSIONS

The adsorption of Li^q (q = -1, 0 or +1), in a low concentration, on different symmetry sites of pristine and defective silicone were studied by DFT calculations. The most stable sites are the H, the SV and the H2 site at the pristine, SV, DV and STW configurations, respectively. The OCV follows the same trend. In all systems, the most stable adsorption energies were found to be when the Li^{+1} ion is considered. Only the SV system presents asymmetric DOS curves with an induced magnetic moment of 1.85 μ_B. The defective cases showed a p-doping behavior as a consequence of the defect states around the Fermi level, which is more visible at the SV system. After Li adsorption, the DOS curves present a shift of the Fermi level towards the conduction band (CB) for the pristine system, while in the case of the SV configurations it is shifted to the VB. In the DV case, for Li^0 and Li^{+1}, there is a shift towards the CB and VB, respectively. The Bader analysis of the lithiated systems shows that there is a local charge

transference from Li to the surface, and that although Li has +1, 0 or -1 charge as a starting point, it always ends up being a Li^{+1} ion on the surface as the most suitable scenario. The QC and charge density analysis in all configurations with and without Li adsorbed show a good agreement with the DOS curves. We found that the addition of defects in the silicene generates an improvement in the positive voltages of the charge density and QC curves, due to the presence of 3p orbitals of Si atoms around the defects. The QC and electron charge densities showed an enhancement after the charged Li adsorption, mainly because of the hybridization of s-p orbitals of the Li-Si bond. An increase in the QC in positive bias for the SV and DV sites is present, being predominant in the Li^{+1} cases. The QC and electron charge density improvements are important parameters to be used in the design of battery anodes. The promising role of charged Li/silicene is also an alternative to other 2D possibilities.

REFERENCES

Ali, M., Pi, X., Liu, Y. and Yang, D. Electronic and magnetic properties of graphene, silicene and germanene with varying vacancy concentration, *AIP Advances* 7: 045308, 2017.

Ayodhya, D. and Veerabhadram G. A brief review on synthesis, properties and lithium-ion battery applications of borophene. *Flatchem* 19:100150(pp. 1-15), 2020.

Bader, R. *Atoms in Molecules: A Quantum Theory*, Oxford University Press, 1990.

Blöchl, P. E. Projector Augmented-Wave Method. *Physical Review B* 50(24):17953-17979, 1994.

Chavan, H.S., Hou, B., Ahmed, A.T.A., Jo, Y., Cho, S., Kim, J., Pawar, S.M., Cha, S.N., Inamdar, A.I., Im, H. and Kim, H. Nanoflake $NiMoO_4$ based smart supercapacitor for intelligent power balance monitoring. *Solar Energy Materials and Solar Cells* 185: 166-173, 2018.

Chowdhury, S. and Jana D. A theoretical review on electronic, magnetic and optical properties of silicene. *Reports on Progress in Physics* 79(12): 126501(pp.1-57), 2016.

Huang, J., Chen, H.J., Wu, M.-S., Liu, C.-Y., Ouyang G. and Xu, B. First-Principles Calculation of Lithium Adsorption and Diffusion on Silicene, *Chinese Physics Letter*s 30 (1): 017103, 2013

Luo, W., Ma, Y., Gong, X. and Xiang, H. Prediction of Silicon-Based Layered Structures for Optoelectronic Applications. *Journal of American Chemical Society* 136 (45): 15992−15997, 2014.

Monkhorst, H. J. and Pack, J. D. Special Points for Brillouin-zone Integrations. *Physical Review B* 13(12): 5188-5192, 1976.

Momeni, M. J., Mousavi-Khoshdel, M. and Leisegang, T. Exploring the performance of pristine and defective silicene and silicene-like XSi_3 (X = Al, B, C, N, P) sheets as supercapacitor electrodes: A density functional theory calculation of quantum capacitance. *Physica E: Low-Dimensional Systems and Nano*structures 124: 114290(pp. 1-7), 2020.

Paek, E., Pak, A. J., Kweon, K. E. and Hwang, G. S. On the origin of the enhanced supercapacitor performance of nitrogen-doped graphene. *The Journal of Physical Chemistry C* 117(11):5610-5616, 2013.

Pattarapongdilok, N and Parasuk, V. Adsorptions of lithium ion/atom and packing of Li ions on graphene quantum dots: Application for Li-ion battery, *Computational and Theoretical Chemistry* 1177: 11279, 2020.

Perdew, J.P., Burke, K. and Ernzerhof, M. Generalized gradient approximation made simple. *Physical Review Letters* 77(18): 3865–3868, 1996.

Sangavi, S., Santhanamoorthi, N., and Vijayakumar, S. Density functional theory study on the adsorption of alkali metal ions with pristine and defected graphene sheet, *Molecular Physics* 117: 462-673, 2019.

Setiadi, J., Arnold, M. D., Ford, M. J. Li-ion adsorption and diffusion on two-dimensional silicon with defects: A first principles study, *ACS Applied Materials and Interfaces* 5 (21): 10690–10695, 2013

Shanmugam, S., Nachimuthu, S. and Subramaniam, V. The effect of edge termination on Li^+ ion adsorption of pristine and defected graphene sheets. *Journal of Material Sci*ence 55: 5920–5937, 2020.

Wang, G., Zhang, L., and Zhang, J., A review of electrode materials for electrochemical supercapacitors. *Chemical Society Reviews* 41(2):797-828, 2012.

Wang, Y. and Li, Y. Ab initio prediction of two-dimensional Si_3C enabling high specific capacity as an anode material for Li/Na/K-ion batteries. *Journal of Materials Chemistry A* 8(8): 4274–4282, 2020.

Xu, Q., Yang, G. M., Fan, X. and Zheng, W. T. Adsorption of metal atoms on silicene: Stability and quantum capacitance of silicene-based electrode materials. *Physical Chemistry Chemical Physics* 21(8): 4276–4285, 2019.

Yang, G.M., Xu, Q., Fan, X. and Zheng, W. T. Quantum Capacitance of Silicene-Based Electrodes from First-Principles Calculations. *The Journal of Physical Chemistry C* 122(4): 1903-1912, 2018.

Yu, Y.-X. Can all nitrogen-doped defects improve the performance of graphene anode materials for lithium-ion batteries? *Phys. Chem. Chem. Phys.* 15: 16819-16827, 2013a.

Yu, Y.-X. Graphenylene: a promising anode material for lithium-ion batteries with high mobility and storage. *Journal of Materials Chemistry A* 1: 13559-13566, 2013b.

Yu, Y.X. Effect of Defects and Solvents on Silicene Cathode of Nonaqueous Lithium-Oxygen Batteries: A Theoretical Investigation. *The Journal of Physical Chemistry C* 123(1): 205−213, 2018.

Zhang, L.L., Zhao, X., Ji, H., Stoller, M.D., Lai, L., Murali, S., Mcdonnell, S., Cleveger, B., Wallace, R.M. and Ruoff, R.S. Nitrogen doping of graphene and its effect on quantum capacitance, and a new insight on the enhanced capacitance of N-doped carbon. *Energy and Environmental Science* 5(11): 9618-9625, 2012.